DOI: 10.1021/ic900874f

Inorganic Chemistry
Article

Synthesis, Characterization, and Electrochemistry of a Series of Iron(II) Complexes Containing Self-Assembled 1,5-Diaza-3,7-diphosphabicyclo[3.3.1]nonane Ligands

Andrew D. Burrows,*,† Ross W. Harrington,‡ Andrew S. Kirk,† Mary F. Mahon,† Frank Marken,† John E. Warren,§ and Michael K. Whittlesey*,†

†*Department of Chemistry, University of Bath, Claverton Down, Bath BA2 7AY, U.K.,* ‡*School of Chemistry, Newcastle University, Newcastle upon Tyne NE1 7RU, U.K., and* §*CLRC Daresbury Laboratory, Daresbury, Warrington WA4 4AD, U.K.*

Received May 6, 2009

The reaction between $PPh(CH_2OH)_2$, iron(II) sulfate, ammonium sulfate, and formaldehyde in aqueous solution gives the iron(II) complex [Fe(κ^2-O_2SO_2)$\mathbf{L}_2$] (**1**), where **L** is the bidentate phosphine ligand 3,7-diphenyl-1,5-diaza-3,7-diphosphabicyclo[3.3.1]nonane. During the course of the reaction, the ligand **L** self-assembles on the metal center. The reaction between $PPh(CH_2OH)_2$, iron(II) chloride, ammonium chloride, and formaldehyde under similar conditions gives *cis*-[$FeCl_2\mathbf{L}_2$] (*cis*-**2**). The complex *cis*-**2** is converted into *trans*-**2** in Et_2O, whereas in water it is converted into *cis*-$[Fe(OH_2)_2\mathbf{L}_2]^{2+}$, though both of these interconversions are reversible. The chloro ligands in *cis*-**2** are readily displaced by reaction with thiocyanate, azide, and carbonate to give *cis*- and *trans*-[$Fe(NCS)_2\mathbf{L}_2$] (*cis*- and *trans*-**3**), *cis*- and *trans*-[$Fe(N_3)_2\mathbf{L}_2$] (*cis*- and *trans*-**4**), and [Fe(κ^2-O_2CO)$\mathbf{L}_2$] (**5**), respectively. The complex *cis*-**2** reacts with CO in water to give *trans*-[FeCl(CO)$\mathbf{L}_2$]Cl (*trans*-**6**), whereas *trans*-**2** reacts with CO in diethyl ether to give *cis*-[FeCl(CO)$\mathbf{L}_2$]Cl (*cis*-**6**), though *cis*-**6** isomerizes in water to form *trans*-**6**. The reaction of *cis*-**2** with sodium borohydride gives the hydride chloride complex *trans*-[FeCl(H)$\mathbf{L}_2$] (**7**). Electrochemical studies have been undertaken on complexes **1**, *cis*-**2**, and **7**. These reveal reversible oxidations for *cis*-**2** and **7**, with the latter giving rise to an unusual 17-electron iron(III) hydride chloride complex. Crystal structures have been obtained for **1**, *trans*-**2**, *trans*-**3**, **5**, and **7**.

Introduction

Despite the emergence of new classes of ligand, tertiary phosphines continue to attract attention as the ready variation of substituents allows these ligands to be tailored to particular uses. Further control of the properties of a metal complex can be obtained using a bi- or poly dentate ligand, as the linkers between the donor atoms affect the bite angle.[1] Despite the potential advantages this control can confer, polydentate and macrocyclic phosphines can be challenging to prepare.[2] Use of a metal template, however, allows such ligands to be prepared in fewer steps and overall higher yields than might otherwise be possible. For example, Edwards and co-workers have used coupling reactions between coordinated primary diphosphines and vinylphosphines to prepare cyclic triphosphines with 9−12 membered rings.[3] Stelzer and co-workers have used a related approach to prepare cyclic tetraphosphines,[4] and also employed the reaction between coordinated secondary diphosphines and diketones to prepare similar products.[5] More recently, Morris and co-workers have shown that template reactions on iron can be used to convert a dimeric phosphonium salt into tridentate PN_2-donor ligands, and subsequently tetradentate P_2N_2-donor ligands.[6]

In 2000 it was reported that an unusual self-assembly reaction takes place between tetrakis(hydroxymethyl)phosphonium sulfate (THPS, $[P(CH_2OH)_4]_2SO_4$), and ammonium sulfate in the

*To whom correspondence should be addressed. E-mail: a.d.burrows@bath.ac.uk; m.k.whittlesey@bath.ac.uk.

(1) van Leeuwen, P. W. N. M.; Kamer, P. C. J.; Reek, J. N. H.; Dierkes, P. *Chem. Rev.* **2000**, *100*, 2741–2770.

(2) Dodds, F.; García, F.; Kowenicki, R. A.; McPartlin, M.; Steiner, A.; Wright, D. S. *Chem. Commun.* **2005**, 3733–3735. Märkl, G.; Zollitsch, T.; Kreitmeier, P.; Prinzhorn, M.; Reithinger, S.; Eibler, E. *Chem.—Eur. J.* **2000**, *6*, 3806–3820. Naumov, R. N.; Karasik, A. A.; Sinyashin, O. G.; Lönnecke, P.; Hey-Hawkins, E. *Dalton Trans.* **2004**, 357–358.

(3) Edwards, P. G.; Newman, P. D.; Hibbs, D. E. *Angew. Chem., Int. Ed.* **2000**, *39*, 2722–2724. Edwards, P. G.; Newman, P. D.; Malik, K. M. A. *Angew. Chem., Int. Ed.* **2000**, *39*, 2922–2924. Edwards, P. G.; Haigh, R.; Li, D.; Newman, P. D. *J. Am. Chem. Soc.* **2006**, *128*, 3818–3830. Battle, A. R.; Edwards, P. G.; Haigh, R.; Hibbs, D. E.; Li, D.; Liddiard, S. M.; Newman, P. D. *Organometallics* **2007**, *26*, 377–386. Edwards, P. G.; Malik, K. M. A.; Ooi, L.; Price, A. J. *Dalton Trans.* **2006**, 433–441. Edwards, P. G.; Whatton, M. L. *Dalton Trans.* **2006**, 442–450.

(4) Brauer, D. J.; Lebbe, T.; Stelzer, O. *Angew. Chem., Int. Ed. Engl.* **1988**, *27*, 438–439. Lebbe, T.; Machnitzki, P.; Stelzer, O.; Sheldrick, W. S. *Tetrahedron* **2000**, *56*, 157–164.

(5) Bartsch, R.; Hietkamp, S.; Morton, S.; Peters, H.; Stelzer, O. *Inorg. Chem.* **1983**, *22*, 3624–3632.

(6) Mikhailine, A. A.; Kim, E.; Dingels, C.; Lough, A. J.; Morris, R. H. *Inorg. Chem.* **2008**, *47*, 6587–6589. Mikhailine, A.; Lough, A. J.; Morris, R. H. *J. Am. Chem. Soc.* **2009**, *131*, 1394–1395.

Published on Web 09/11/2009

Scheme 1

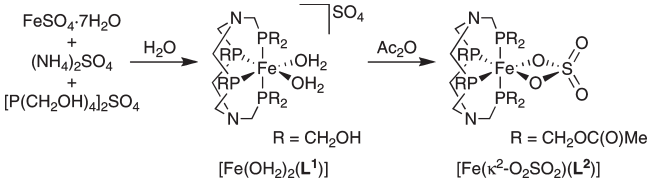

presence of iron(II) sulfate to form $[Fe(OH_2)_2(\mathbf{L^1})]SO_4$, which contains an unusual tetraphosphine ligand (Scheme 1).[7] THPS is used as a biocide in oil wells, and this product was first detected in the red coloration of water from these systems. In the oil wells, the source of the metal was iron sulfide deposits, which are dissolved by THPS. We have previously reported ligand substitution reactions on $[Fe(OH_2)_2(\mathbf{L^1})]SO_4$ and also the esterification of the hydroxymethyl groups on reaction with acetic anhydride which converts $[Fe(OH_2)_2(\mathbf{L^1})]SO_4$ to $[Fe(\kappa^2\text{-}O_2SO_2)(\mathbf{L^2})]$ (Scheme 1).[8]

Reactions between bis(hydroxymethyl)phosphines and amines have been studied in the absence of templates. In 1980, Märkl and co-workers showed that reactions between an alkyl or aryl bis(hydroxymethyl)phosphine, $PR(CH_2OH)_2$, and a primary amine led to 1,5-diaza-3,7-diphosphacyclooctanes.[9] Subsequently, these eight-membered rings have been prepared with a wide range of substituents, including chiral centers,[10] ferrocenyl groups,[11] and amino acids.[12,13] The amine used in the synthesis is crucial to determining the nature of the product formed. Karasik, Hey-Hawkins, and co-workers found that they could obtain linear bis(arylaminomethyl)phosphines, six-membered 1,3-diaza-5-phosphacyclohexanes and 1,5-diaza-3,7-diphosphacyclooctanes from aryl bis(hydroxymethyl)phosphines.[14] Katti and co-workers have also investigated the reactions of a number of hydroxymethyl phosphines with primary amines. They showed that the reactions between 1,2-bis(bis(hydroxymethyl)phosphino)ethane and amino acids gave 3,7-diaza-1,5-diphosphabicyclo[3.3.2]decanes.[12,15]

Our objective in this work was to assess the generality of the self-assembly reaction that produces $[Fe(OH_2)_2(\mathbf{L^1})]SO_4$ by changing the phosphorus source from tetrakis(hydroxymethyl)phosphonium to a bis(hydroxymethyl)phosphine. In this paper, we report our results using $PPh(CH_2OH)_2$.

Experimental Section

Reactions were typically carried out in air, though manipulations on a Schlenk line under dinitrogen were used as indicated. $PPh(CH_2OH)_2$ was prepared as previously reported.[16] All other chemicals were obtained commercially and used without further purification. NMR spectra were recorded at 298 K on Bruker Avance 300, 400, and 500 MHz NMR spectrometers, and referenced to residual protio solvent signals for ^{1}H NMR spectra (D_2O, δ 4.80; $CDCl_3$, δ 7.24; C_6D_6, δ 7.15) and to solvent resonances for $^{13}C\{^1H\}$ NMR (D_2O + 1% MeOH, δ 49.5; $CDCl_3$ δ 77.2). $^{31}P\{^1H\}$ NMR chemical shifts were referenced externally to 85% H_3PO_4. Microanalyses were carried out by Mr. Alan Carver at the University of Bath. IR spectra were recorded as KBr discs on a Nicolet Nexus FTIR spectrometer. Mass spectra were recorded on a Bruker MicrOTOF electrospray time-of-flight (ESI-TOF) mass spectrometer (Bruker Daltonik GmbH) coupled to an Agilent 1200 LC system (Agilent Technologies).

Synthesis of $[Fe(\kappa^2\text{-}O_2SO_2)L_2]$ (1). Iron(II) sulfate heptahydrate (0.101 g, 0.363 mmol), ammonium sulfate (0.097 g, 0.734 mmol), and formaldehyde (0.066 g of a 37% aq. solution, 0.813 mmol) were dissolved in water (20 mL) under an atmosphere of N_2 to give a pale green solution. $PPh(CH_2OH)_2$ (0.247 g, 1.45 mmol) was separately dissolved in degassed water (10 mL), which was then slowly added dropwise over 30 min to the iron-containing solution while stirring, taking care to keep the pH below 5.5. The addition of the aqueous phosphine solution gave rise to a purple coloration of the solution, which increased in intensity with further addition of the phosphine solution. As the solution became darker, a purple solid began to precipitate. After the addition of $PPh(CH_2OH)_2$ was complete, the reaction mixture was left to stir for 1 h, after which the purple product was collected by filtration and washed with cold water (2 mL). The purple solid of **1** was then dried in a desiccator under reduced pressure overnight. Yield 0.093 g (33%). ^{1}H NMR (500 MHz, $CDCl_3$): δ 7.4−7.1 (m, 20H, Ar), 5.27 (d, 2H, PCH_2N AB1, $\Delta\nu$ 821 Hz, $^2J_{HH}$ 13.9 Hz), 4.92 (d, 2H, PCH_2N AB2, $\Delta\nu$ 736 Hz, $^2J_{HH}$ 12.9 Hz), 4.17 (d, 2H, NCH_2N AB, $\Delta\nu$ 76 Hz, $^2J_{HH}$ 13.9 Hz), 4.01 (d, 2H, NCH_2N AB, $\Delta\nu$ 76 Hz, $^2J_{HH}$ 13.9 Hz), 4.03 (d, 2H, PCH_2N AB3, $\Delta\nu$ 228 Hz, $^2J_{HH}$ 13.9 Hz), 3.63 (d, 2H, PCH_2N AB1, $\Delta\nu$ 821 Hz, $^2J_{HH}$ 13.9 Hz), 3.53 (d, 2H, PCH_2N AB4, $\Delta\nu$ 411 Hz, $^2J_{HH}$ 13.9 Hz), 3.53 (d, 2H, PCH_2N AB3, $\Delta\nu$ 228 Hz, $^2J_{HH}$ 13.9 Hz), 3.45 (d, 2H PCH_2N AB2, $\Delta\nu$ 736 Hz, $^2J_{HH}$ 12.9 Hz), 2.71 (d, 2H, PCH_2N AB4, $\Delta\nu$ 411 Hz, $^2J_{HH}$ 13.9 Hz). $^{31}P\{^1H\}$ (122 MHz, $CDCl_3$): δ −26.4 (t, $^2J_{PP}$=72 Hz), −51.2 (t, $^2J_{PP}$ = 72 Hz). Found: C, 50.7; H, 5.25; N, 6.28%. Calcd for $C_{34}H_{40}N_4O_4FeP_4S\cdot H_2O$: C, 51.1; H, 5.30; N, 6.99%. MS (ESI): m/z = 803.1 $[M + Na]^+$.

Synthesis of *cis*-$[FeCl_2L_2]$ (*cis*-2) and *trans*-$[FeCl_2L_2]$ (*trans*-2). Iron(II) chloride tetrahydrate (0.335 g, 1.69 mmol), NH_4Cl (0.362 g, 6.77 mmol), and formaldehyde (0.281 g of a 37% aq. solution, 3.46 mmol) were dissolved in water (25 mL). $PPh(CH_2OH)_2$ (1.150 g, 6.76 mmol) was dissolved in degassed water (9 mL), then added dropwise over 45 min to the iron-containing solution while stirring, taking care to keep the pH below 5. The reaction mixture was stirred for 2 h, then the purple product was collected by filtration and washed with cold water (2 mL). The purple solid of *cis*-**2** was dried in a desiccator under reduced pressure overnight. Yield 1.01 g (79%). $^{31}P\{^1H\}$ NMR (122 MHz, $CDCl_3$): δ −32.4 (br t), −46.5 (br t). $^{31}P\{^1H\}$ NMR (122 MHz, D_2O): δ −17.9 (m, $^2J_{PP}$ 74 Hz), −38.2 (m, $^2J_{PP}$ 74 Hz). A sample of *cis*-**2** was placed in a cellulose extraction thimble inserted into a Soxhlet extractor fitted with a condenser and round-bottomed flask. Diethyl ether was placed in the round-bottomed flask and heated to reflux for 24 h. This gave a yellow solution, which yielded yellow crystals of *trans*-**2** upon evaporation of the diethyl ether solution at room temperature. Found: C, 53.4; H, 5.33; N, 7.23%. Calcd for $C_{34}H_{40}N_4FeP_4Cl_2$: C, 54.0; H, 5.34; N, 7.42%. MS (ESI): m/z 684.2 $[M - 2Cl]^+$.

(7) Jeffery, J. C.; Odell, B.; Stevens, N.; Talbot, R. E. *Chem. Commun.* **2000**, 101–102.
(8) Burrows, A. D.; Dodds, D.; Kirk, A. S.; Lowe, J. P.; Mahon, M. F.; Warren, J. E.; Whittlesey, M. K. *Dalton Trans.* **2007**, 570–580.
(9) Märkl, G.; Jin, G. Y.; Schoerner, C. *Tetrahedron Lett.* **1980**, *21*, 1409–1412.
(10) Karasik, A. A.; Naumov, R. N.; Sinyashin, O. G.; Belov, G. P.; Novikova, H. V.; Lönnecke, P.; Hey-Hawkins, E. *Dalton Trans.* **2003**, 2209–2214.
(11) Karasik, A. A.; Spiridonova, Y. S.; Yakhvarov, D. G.; Sinyashin, O. G.; Lönnecke, P.; Sommer, R.; Hey-Hawkins, E. *Mendeleev Commun.* **2005**, 89–90.
(12) Berning, D. E.; Katti, K. V.; Barnes, C. L.; Volkert, W. A. *J. Am. Chem. Soc.* **1999**, *121*, 1658–1664.
(13) Karasik, A. A.; Sinyashin, O. G.; Heinicke, J.; Hey-Hawkins, E. *Phosphorus, Sulfur Silicon Relat. Elem.* **2002**, *177*, 1469–1471.
(14) Karasik, A. A.; Naumov, R. N.; Sommer, R.; Sinyashin, O. G.; Hey-Hawkins, E. *Polyhedron* **2002**, *21*, 2251–2256.
(15) Katti, K. V.; Kannan, R.; Katti, K. K.; Pillarsetty, N.; Barnes, C. L. *Phosphorus, Sulfur Silicon Relat. Elem.* **2002**, *177*, 1587–1589.
(16) Higham, L. J.; Whittlesey, M. K.; Wood, P. T. *Dalton Trans.* **2004**, 4202–4208.

Synthesis of *cis*-[Fe(NCS)$_2$L$_2$] (*cis*-3) and *trans*-[Fe(NCS)$_2$L$_2$] (*trans*-3). Compound *cis*-**2** (0.050 g, 0.66 mmol) was added to EtOH (10 mL) giving a purple suspension. Excess potassium thiocyanate (0.129 g, 1.33 mmol) was added to the reaction mixture giving an orange precipitate of *cis*-**3**. The orange solid was collected by filtration and washed with cold water (5 mL). Yield 0.043 g (78%). Single crystals of *trans*-**3** suitable for X-ray diffraction were grown from a $CDCl_3$ solution over 48 h. $^{31}P\{^1H\}$ and ^1H NMR spectroscopy showed a mixture of *cis*-**3** and *trans*-**3** in an 4:1 ratio after 20 min in solution, which changed to a 2:3 ratio after 48 h. ^1H NMR (*cis*-**3**) (300 MHz, $CDCl_3$): δ 7.8−6.6 (m, 20H, Ar), 4.6 (d, 2H, PCH_2N AB1, $\Delta\nu$ 391 Hz, $^2J_{HH}$ 13.9 Hz), 4.3 (d, 2H, PCH_2N AB2, $\Delta\nu$ 387 Hz, $^2J_{HH}$ 13.4 Hz), 4.0 (d, 2H, PCH_2N AB3, $\Delta\nu$ 161 Hz, $^2J_{HH}$ 13.8 Hz), 3.9 (d, 2H, NCH_2N AB, $\Delta\nu$ 24 Hz, $^2J_{HH}$ 13.9 Hz), 3.8 (d, 2H, NCH_2N AB, $\Delta\nu$ 24 Hz, $^2J_{HH}$ 13.9 Hz), 3.5 (d, 2H, PCH_2N AB4, $\Delta\nu$ 309 Hz, $^2J_{HH}$ 13.8 Hz), 3.5 (d, 2H, PCH_2N AB3, $\Delta\nu$ 161 Hz, $^2J_{HH}$ 13.8 Hz), 3.3 (d, 2H, PCH_2N AB1, $\Delta\nu$ 391 Hz, $^2J_{HH}$ 13.9 Hz), 3.0 (d, 2H PCH_2N AB2, $\Delta\nu$ 387 Hz, $^2J_{HH}$ 13.4 Hz), 2.4 (d, 2H, PCH_2N AB4, $\Delta\nu$ 309 Hz, $^2J_{HH}$ 13.8 Hz). $^{31}P\{^1H\}$ (*cis*-**3**) (122 MHz, $CDCl_3$): δ −31.0 (m, $^2J_{PP}$ 77 Hz), −38.6 (m, $^2J_{PP}$ 77 Hz). ^1H NMR (*trans*-**3**) (300 MHz, $CDCl_3$): δ 7.8−6.6 (m, 20H, Ar), 4.3 (d, 8H, PCH_2N AB, $\Delta\nu$ 221 Hz, $^2J_{HH}$ 13.4 Hz), 4.0 (s, 4H, NCH_2N), 3.5 (d, 8H, PCH_2N AB, $\Delta\nu$ 221 Hz, $^2J_{HH}$ 13.4 Hz). $^{31}P\{^1H\}$ (*trans*-**3**) (122 MHz, $CDCl_3$): δ −42.2 (s). IR (cm^{-1}): 2098 (ν_{NCS}). MS (ESI): *m*/*z* 742.1304 (Calcd for $[M - NCS]^+$, *m*/*z* 742.1304).

Synthesis of *cis*-[Fe(N$_3$)$_2$L$_2$] (*cis*-4) and *trans*-[Fe(N$_3$)$_2$L$_2$] (*trans*-4). Compound *cis*-**2** (0.050 g, 0.066 mmol) was added to EtOH (10 mL) giving a purple suspension. Excess NaN_3 (0.086 g, 1.32 mmol) was added to the reaction mixture, to give a red suspension of *cis*-**4**. The red solid was collected by filtration and washed with cold water (5 mL). Repeated recrystallizations from various solvent combinations failed to give a satisfactory microanalysis because of the difficulty in removing excess sodium azide from the product. $^{31}P\{^1H\}$ and ^1H NMR spectroscopy showed a mixture of *cis*-**4** and *trans*-**4** in an 11:1 ratio, which did not change over time. ^1H NMR (*cis*-**4**) (300 MHz, $CDCl_3$): δ 7.5−7.1 (m, 20H, Ar), 4.7 (d, 2H, PCH_2N AB1, $\Delta\nu$ 30 Hz, $^2J_{HH}$ 13.6 Hz), 4.6 (d, 2H, PCH_2N AB2, $\Delta\nu$ 473 Hz, $^2J_{HH}$ 13.6 Hz), 3.9 (d, 2H, PCH_2N AB3, $\Delta\nu$ 155 Hz, $^2J_{HH}$ 13.6 Hz), 3.9 (d, 2H, NCH_2N AB, $\Delta\nu$ 25 Hz, $^2J_{HH}$ 13.6 Hz,), 3.9 (d, 2H, NCH_2N AB, $\Delta\nu$ 25 Hz, $^2J_{HH}$ 13.6 Hz,), 3.5 (d, 2H, PCH_2N AB4, $\Delta\nu$ 293 Hz, $^2J_{HH}$ 13.6 Hz), 3.4 (d, 2H, PCH_2N AB3, $\Delta\nu$ 155 Hz, $^2J_{HH}$ 13.6 Hz), 3.4 (d, 2H, PCH_2N AB1, $\Delta\nu$ 30 Hz, $^2J_{HH}$ 13.6 Hz), 3.0 (d, 2H, PCH_2N AB2, $\Delta\nu$ 473 Hz, $^2J_{HH}$ 13.6 Hz), 2.5 (d, 2H, PCH_2N AB4, $\Delta\nu$ 293 Hz, $^2J_{HH}$ 13.6 Hz). $^{31}P\{^1H\}$ (*cis*-**4**) (122 MHz, $CDCl_3$): δ −27.4 (m, $^2J_{PP}$ 75 Hz), −36.9 (m, $^2J_{PP}$ 75 Hz). ^1H NMR (*trans*-**4**) (300 MHz, $CDCl_3$): δ 7.5−7.1 (m, 20H, Ar), 4.3 (d, 8H, PCH_2N AB, $\Delta\nu$ 186 Hz, $^2J_{HH}$ 14.1 Hz), 4.2 (s, 4H, NCH_2N), 3.6 (d, 8H, PCH_2N AB, $\Delta\nu$ 186 Hz, $^2J_{HH}$ 14.1 Hz). $^{31}P\{^1H\}$ (*trans*-**4**) (122 MHz, $CDCl_3$): δ −43.2 (s). IR (cm^{-1}): 2043 (ν_{N3}). MS (ESI): *m*/*z* 684.2 $[M - 2N_3]^+$.

Synthesis of [Fe(κ^2-O$_2$CO)L$_2$] (5). Compound *cis*-**2** (0.107 g, 0.142 mmol) was added to ethanol (20 mL) giving a purple suspension. Excess sodium carbonate (0.170 g, 1.60 mmol) in water (5 mL) was added, to give a pink suspension. The resulting pink solid was separated by filtration and recrystallized from chloroform. Yield 0.061 g (59%). Single crystals of **5** suitable for X-ray diffraction grew from an aqueous solution over 8 weeks. ^1H NMR (500 MHz, $CDCl_3$): δ 7.6−7.1 (m, 20H, Ar), 5.16 (d, 2H, PCH_2N AB1, $\Delta\nu$ 918 Hz, $^2J_{HH}$ 12.9 Hz,), 4.76 (d, 2H, PCH_2N AB2, $\Delta\nu$ 680 Hz, $^2J_{HH}$ 12.9 Hz), 4.03 (d, 2H, PCH_2N AB3, $\Delta\nu$ 277 Hz, $^2J_{HH}$ 12.9 Hz,), 4.00 (d, 2H, NCH_2N AB, $\Delta\nu$ 33 Hz, $^2J_{HH}$ 14.5 Hz), 3.94 (d, 2H, NCH_2N AB, $\Delta\nu$ 33 Hz, $^2J_{HH}$ 13.9 Hz), 3.48 (d, 2H, PCH_2N AB4, $\Delta\nu$ 401 Hz, $^2J_{HH}$ 13.9 Hz), 3.48 (d, 2H, PCH_2N AB3, $\Delta\nu$ 277 Hz, $^2J_{HH}$ 12.9 Hz), 3.40 (d, 2H, PCH_2N AB2, $\Delta\nu$ 680 Hz, $^2J_{HH}$ 12.9 Hz), 3.32 (d, 2H, PCH_2N AB1, $\Delta\nu$ 918 Hz, $^2J_{HH}$ 12.9 Hz), 2.68 (d, 2H, PCH_2N AB4, $\Delta\nu$ 401 Hz, $^2J_{HH}$ 13.9 Hz). $^{31}P\{^1H\}$ (122 MHz, $CDCl_3$): δ −20.2 (t, $^2J_{PP}$ 72 Hz), −41.4 (t, $^2J_{PP}$ 72 Hz). $^{13}C\{^1H\}$ (125 MHz, $CDCl_3$): δ 163.7 (s, O_2CO), 131−128 (m, Ar), 72.8 (s, NCH_2N), 53.3 (m, PCH_2N), 51.2 (m, PCH_2N), 50.9 (s, PCH_2N), 48.0 (s, PCH_2N). Calcd for $C_{35}H_{40}N_4O_3FeP_4$: C, 56.5; H, 5.42; N, 7.53%. Found: C, 56.1; H, 5.29; N, 7.46%. IR (cm^{-1}): 1556 (ν_{CO_3}). MS (ESI): *m*/*z* 744.1678. (Calcd for $[M]^+$, *m*/*z* 744.1400).

Synthesis of *trans*-[FeCl(CO)L$_2$]Cl (*trans*-6). Compound *cis*-**2** (0.100 g, 0.133 mmol) was dissolved in H_2O (20 mL) and CO bubbled through the solution for 20 min. The reaction was stirred for 2 h, resulting in a yellow solution. A yellow solid was precipitated from solution by the addition of acetone. The yellow solid of *trans*-**6** was washed with additional acetone (5 mL) and dried in a desiccator. Yield 0.087 g (83%). ^1H NMR (400 MHz, D_2O): δ 7.1−6.9 (m, 20H, Ar), 4.9 (d, 4H, PCH_2N AB1, $\Delta\nu$ 423 Hz, $^2J_{HH}$ 13.5 Hz), 4.4 (d, 4H, PCH_2N AB2, $\Delta\nu$ 156 Hz, $^2J_{HH}$ 14.5 Hz), 3.9 (s, 4H, NCH_2N), 3.8 (d, 4H, PCH_2N AB2, $\Delta\nu$ 156 Hz, $^2J_{HH}$ 14.5 Hz), 3.5 (d, 4H, PCH_2N AB1, $\Delta\nu$ 423 Hz, $^2J_{HH}$ 13.5 Hz). $^{31}P\{^1H\}$ (122 MHz, D_2O): δ −51.0 (s). $^{13}C\{^1H\}$ (*trans*-[FeCl(^{13}CO)L$_2$]Cl, 126 MHz, D_2O): δ 214.7 (quintet, ^{13}CO, $^2J_{CP}$ 25.8 Hz), 132−129 (m, Ar), 72.2 (s, NCH_2N), 52.3 (s, PCH_2N), 49.1 (s, PCH_2N). Calcd for $C_{35}H_{40}N_4OFeP_4Cl_2 \cdot 6H_2O$: C, 46.6; H, 5.81; N, 6.21%. Found: C, 46.3; H, 5.47; N, 6.06%. IR (cm^{-1}): 1939 ($\nu_{^{12}CO}$), 1895 ($\nu_{^{13}CO}$). MS (ESI): *m*/*z* 747.1165. (Calcd for $[M]^+$, *m*/*z* 747.1191).

Synthesis of *cis*-[FeCl(CO)L$_2$]Cl (*cis*-6). Compound *trans*-**2** (0.010 g, 0.013 mmol) was dissolved in diethyl ether (20 mL) giving a pale yellow solution. CO was bubbled through the reaction mixture for 20 min, and the reaction mixture was stirred for a further 4 h, after which time a pale orange precipitate began to form. *cis*-**6** was separated by filtration after a further 7 days of stirring, then washed with Et_2O (5 mL) and dried in air. Yield 0.005 g (48%). Alternatively, *cis*-**6** could be also prepared by addition of 1 atm CO to a $CDCl_3$ solution of *cis*-**2**. $^{31}P\{^1H\}$ NMR (122 MHz, $CDCl_3$): δ −39.4 (ddd, $^2J_{PP}$ 91, 38, 45 Hz), −55.3 (ddd, $^2J_{PP}$ 91, 61, 48 Hz), −59.4 (ddd, $^2J_{PP}$ 38, 61, 120 Hz), −69.0 (ddd, $^2J_{PP}$ 45, 48, 120 Hz). Selected $^{13}C\{^1H\}$ (126 MHz, $CDCl_3$): δ 214.2 (m, ^{13}CO, *J* 20.6 Hz). IR (cm^{-1}): 1974 (ν_{CO}). MS (ESI): *m*/*z* 747.1 $[M]^+$.

Synthesis of *trans*-[FeCl(H)L$_2$] (7). Compound *cis*-**2** (0.200 g, 0.265 mmol) and $NaBH_4$ (0.020 g, 0.529 mmol) were placed in a Schlenk tube under dinitrogen, to which was added degassed EtOH (10 mL), dissolving the starting materials to give an orange solution. Upon stirring for 1 h, an orange suspension of **7** formed. The solution was filtered by cannula under dinitrogen, and the solid washed with degassed ethanol (5 mL) then recrystallized from degassed benzene. Yield 0.128 g (67%). ^1H NMR (400 MHz, C_6D_6): δ 7.0−6.8 (m, 20H, Ar), 5.5 (d, 4H, PCH_2N AB1, $\Delta\nu$ 806 Hz, $^2J_{HH}$ 12.9 Hz), 3.9 (s, 4H, NCH_2N), 3.9 (d, 4H, PCH_2N AB2, $\Delta\nu$ 107 Hz, $^2J_{HH}$ 13.3 Hz), 3.6 (d, 4H, PCH_2N AB2, $\Delta\nu$ 107 Hz, $^2J_{HH}$ 13.3 Hz), 3.5 (d, 4H, PCH_2N AB1, $\Delta\nu$ 806 Hz, $^2J_{HH}$ 12.9 Hz), −28.6 (quintet, FeH, $^2J_{HP}$ 49 Hz). ^{31}P (162 MHz, C_6D_6): δ −27.5 (d, $^2J_{PH}$ = 49 Hz). MS (ESI): *m*/*z* 685.1632. (Calcd for $[M - Cl]^+$, *m*/*z* 685.1632).

Electrochemistry. All reagents used for electrochemical analyses were of analytical or electrochemical grade purity. The supporting electrolyte was tetrabutylammonium hexafluorophosphate in acetonitrile and 1,2-dichloroethane solutions. The solvents were purged with argon prior to use. All experiments were conducted at 295 ± 2 K. Voltammetric experiments were performed using an Ecochemie Autolab potentiostat. For the purpose of these experiments a three electrode cell setup was used, composed of working, counter, and reference electrodes. The working electrode used was a 3 mm diameter platinum electrode unless otherwise stated. The counter electrode consisted of a spiral of platinum wire. All potentials were referenced to internal cobaltocenium hexafluorophosphate, which was referenced to ferrocene ($E_{1/2}$ = 0.00 V) but were measured using a platinum wire pseudo reference (a platinum wire which was immersed and equilibrated in the electrolyte containing solvent used for the experiment).

Table 1. Crystal Data and Structure Refinement for Compounds **1**·2H_2O, *trans*-**2**, *trans*-**3**, **5**·7H_2O, and **7**·1.5C_6H_6

compound	**1**·2H_2O	*trans*-**2**	*trans*-**3**	**5**·7H_2O	**7**·1.5C_6H_6
empirical formula	$C_{34}H_{44}FeN_4O_6P_4S$	$C_{34}H_{40}Cl_2FeN_4P_4$	$C_{36}H_{40}FeN_6P_4S_2$	$C_{35}H_{54}FeN_4O_{10}P_4$	$C_{43}H_{50}ClFeN_4P_4$
formula weight	816.52	755.37	800.59	870.55	838.05
T/K	150(2)	150(2)	150(2)	150(2)	150(2)
wavelength/Å	0.69040	0.71073	0.69070	0.71073	0.68840
crystal system	monoclinic	monoclinic	orthorhombic	triclinic	monoclinic
space group	$C2/c$	$P2_1/c$	$Pbcn$	$P\bar{1}$	$C2/c$
a/Å	15.422(3)	21.9030(2)	15.0527(9)	9.4170(2)	26.873(3)
b/Å	9.5514(18)	10.3800(1)	14.9361(9)	10.5490(2)	14.5374(17)
c/Å	24.333(5)	22.1870(2)	16.0794(9)	22.2750(6)	22.100(3)
α/deg	90	90	90	87.925(1)	90
β/deg	100.469(2)	97.990(1)	90	79.223(1)	111.244(1)
γ/deg	90	90	90	65.600(1)	90
U/Å^3	3524.5(11)	4995.32(8)	3615.1(4)	1977.53(8)	8047.0(17)
Z	4	6	4	2	8
D_c/g cm^{-3}	1.539	1.507	1.471	1.462	1.383
μ/mm^{-1}	0.721	0.838	0.747	0.604	0.637
F(000)	1704	2352	1664	916	3512
crystal size/mm	0.03 × 0.03 × 0.01	0.45 × 0.30 × 0.25	0.07 × 0.01 × 0.01	0.25 × 0.15 × 0.05	0.02 × 0.01 × 0.01
θ min., max for data	3.65,22.55.	3.58, 27.49	3.09, 29.56	3.97, 27.54 .	3.44, 23.91
index ranges	$-16 \le h \le 17$; $-10 \le k \le 9$; $-21 \le l \le 26$	$-27 \le h \le 28$; $-13 \le k \le 13$; $-28 \le l \le 28$	$-21 \le h \le 21$; $-17 \le k \le 21$; $-22 \le l \le 22$	$-12 \le h \le 12$; $-13 \le k \le 12$; $-28 \le l \le 28$	$-31 \le h \le 31$; $-17 \le k \le 17$; $-26 \le l \le 26$
reflections collected	7752	63320	28014	23946	27709
independent reflections, R_{int}	2513, 0.0981	11444, 0.0482	5481, 0.0564	8787, 0.0707	6833, 0.1122
reflections observed ($>2\sigma$)	1549	9117	4240	6814	3746
absorption correction	multiscan	multiscan	multiscan	multiscan	multiscan
max., min transmission	0.991, 0.975	0.80, 0.94	0.981, 0.923	0.9704, 0.8637	0.995, 0.978
data/restraints/parameters	2513/3/233	11444/0/604	5481/0/222	8787/21/529	6833/1/516
goodness-of-fit (F^2)	0.977	1.044	1.014	1.128	0.958
final $R1$, $wR2$ [$I > 2\sigma(I)$]	0.0525, 0.1130	0.0328, 0.0713	0.0343, 0.0792	0.0618, 0.1406	0.0562, 0.1229
final $R1$, $wR2$ (all data)	0.1067, 0.1327	0.0501, 0.0784	0.0525, 0.0868	0.0835, 0.1517	0.1217, 0.1530
largest diff. peak, hole/e Å^{-3}	0.347, −0.364	0.472, −0.427	0.468, −0.402	0.784, −0.691	0.690, −0.312

Crystallography. Single crystals of compounds *trans*-**2** and **5** were analyzed using a Nonius Kappa CCD diffractometer, while the data sets for **1**, *trans*-**3**, and **7** were obtained at Daresbury (Station 9.8 or 16.2 SMX). Details of the data collections, solutions and refinements are given in Table 1. The structures were solved using SHELXS-97 and refined using full-matrix least-squares in SHELXL-97.[17] Refinements were generally straightforward with the following exceptions and points of note. The crystals for **1** and **7** were small, even by Daresbury standards, and this is reflected in the upper Bragg limits for these data collections. Solvent water hydrogens were located in both **1** and **5**, and refined at a distance of 0.9 Å from the relevant parent oxygen in addition to restraining the H···H distances therein to a value of 1.5 Å. In **1**, the asymmetric unit was seen to comprise half of one molecule (with the central metal and sulfur atoms located on a crystallographic 2-fold rotation axis) plus one full water molecule. The asymmetric unit in *trans*-**2**, on the other hand, consists of one full molecule of the iron complex plus half of an additional complex molecule. The central metal in the latter is located on a crystallographic inversion center. Carbons 6−11 were refined after accounting for disorder over two positions in 60:40 ratio. As observed in **1**, the asymmetric unit in *trans*-**3** was also seen to be half of a molecule, with the iron located on a 2-fold rotation axis implicit in the space group. Finally, in **7**, H1 and H2 were located and refined subject to being similar distances from the iron centers to which they respectively bond. The asymmetric unit in this structure contains two crystallographically independent halves of the iron complex (wherein the iron, chloride, and hydride in each are located on a 2-fold rotation axis), one-half of a benzene molecule with full occupancy (proximate to an inversion center) plus an additional molecule of benzene exhibiting 1:1 disorder. The disordered portions of the latter fragments were treated as rigid hexagons in the final least-squares cycles.

(17) Sheldrick, G. M. *Acta Crystallogr., Sect. A* **1990**, *46*, 467–473. Sheldrick, G. M. *SHELXL-97, Computer Program for Crystal Structure Refinement*; University of Göttingen: Göttingen, Germany, 1997.

Results and Discussion

To assess the effects of the phosphine substituents on the self-assembly of the tetraphosphine ligand around the iron center, we sought to undertake analogous reactions to that between $P(CH_2OH)_4^+$ and NH_4^+, but using phosphonium cations of the type $PR(CH_2OH)_3^+$ (R = aryl, alkyl). Since $[Fe(OH_2)_2(\mathbf{L^1})]SO_4$ can also be prepared from $P(CH_2OH)_3$,[7] we reasoned it would be possible to use a bis(hydroxymethyl)phosphine such as $PPh(CH_2OH)_2$ rather than the phosphonium $PPh(CH_2OH)_3^+$, which would be prepared from it. In addition, since $PPh(CH_2OH)_3^+$ would be present in solution in equilibrium with $PPh(CH_2OH)_2$ and HCHO, we decided to investigate the reactions of iron(II) salts with $PPh(CH_2OH)_2$ in the presence of formaldehyde.

Synthesis of $[Fe(\kappa^2\text{-}O_2SO_2)L_2]$ (1). Bis(hydroxymethyl)phenylphosphine, $PPh(CH_2OH)_2$, was prepared via the reaction of phenylphosphine and formaldehyde.[16] An aqueous solution of $PPh(CH_2OH)_2$ was slowly added to an aqueous solution containing iron(II) sulfate, ammonium sulfate, and formaldehyde. The pale green solution rapidly turned purple, and subsequently yielded a purple precipitate. The pH of the reaction solution was monitored and kept below pH 5.5 by adding the phosphine slowly to prevent base-induced decomposition of the products. The purple material **1** was found to be soluble in chloroform, dichloromethane, and acetone, but insoluble in THF and benzene.

Single crystals suitable for X-ray analysis were grown from the slow evaporation of a dichloromethane solution of **1**. The crystallographic analysis showed that **1** does not contain a ligand analogous to that in $[Fe(OH_2)_2(\mathbf{L^1})]SO_4$, but instead **1** has the formula $[Fe(\kappa^2\text{-}O_2SO_2)\mathbf{L}_2]$, where **L** is the new bidentate phosphine ligand 3,7-diphenyl-1,

Scheme 2

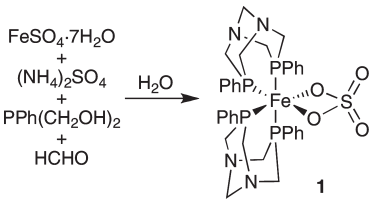

Table 2. Selected Bond Lengths (Å) and Angles (deg) for $1\cdot 2H_2O$[a]

Fe(1)−P(1)	2.2831(16)	S(1)−O(1)	1.501(4)
Fe(1)−P(2)	2.1837(18)	S(1)−O(2)	1.451(4)
Fe(1)−O(1)	2.061(4)		
P(2)−Fe(1)−P(1)	83.42(6)	P(2)−Fe(1)−P(2)′	99.55(10)
P(2)′−Fe(1)−P(1)	98.54(6)	O(1)′−Fe(1)−O(1)	68.4(2)
P(1)−Fe(1)−P(1)′	176.99(11)		

[a] Primed atoms generated by the symmetry operation $-x, y, -z + {}^1/_2$.

5-diaza-3,7-diphosphabicyclo[3.3.1]nonane (Scheme 2). The diphosphine contains two fused six-membered PN_2C_3 rings, with the rings sharing the two nitrogen atoms and the interlinking methylene group. Details of the crystal structure are given below. Following the X-ray structural analysis, the ratio of $PPh(CH_2OH)_2/FeSO_4/(NH_4)_2SO_4/HCHO$ in the synthesis was adjusted to 4:1:2:2 to match the stoichiometry of the product and give an optimal yield.

The $^{31}P\{^1H\}$ NMR spectrum of **1** showed two triplet resonances at δ −26.4 and δ −51.2, with a coupling constant of $^2J_{PP}$ 72 Hz. This pattern is characteristic of the *cis* arrangement of the diphosphine ligands. The ^1H NMR spectrum showed five different AB patterns arising from the five methylene proton environments, four from the P−CH_2−N groups and one from the N−CH_2−N group. This means that all 10 methylene protons on the ligand backbone are inequivalent. The N−CH_2−N methylene protons give rise to the AB system centered at δ 4.1, though it is difficult to unambiguously assign the four remaining AB systems to particular methylene groups. The ESI mass spectrum of **1** shows a major peak at m/z 803.1, which corresponds to $[M + Na]^+$.

The diphosphine ligand **L** can be thought of as a 1, 5-diaza-3,7-diphosphacyclooctane with a methylene bridge between the two nitrogen atoms. This bridging CH_2 moiety is formed from the condensation of a formaldehyde molecule with an N−H bond on each side of the eight-membered ring, which means that the formaldehyde plays two roles in the self-assembly of the diphosphine ligand—it acts as a catalyst in the Mannich reaction involved in the self-assembly process, as well as a reagent which is an essential part of the final ligand structure.

X-ray Crystal Structure of $[Fe(\kappa^2\text{-}O_2SO_2)L_2]\cdot 2H_2O$ ($1\cdot 2H_2O$). The crystallographic analysis revealed that the crystals were of the dihydrate, $1\cdot 2H_2O$. The asymmetric unit contains one-half of the complex molecule and a molecule of H_2O, with the remainder of the formula unit generated by symmetry. Selected bond lengths and angles for $1\cdot 2H_2O$ are given in Table 2. The iron(II) center has a distorted octahedral geometry and is coordinated to two bidentate **L** ligands, arranged in a *cis* configuration, and a bidentate sulfato ligand, as shown

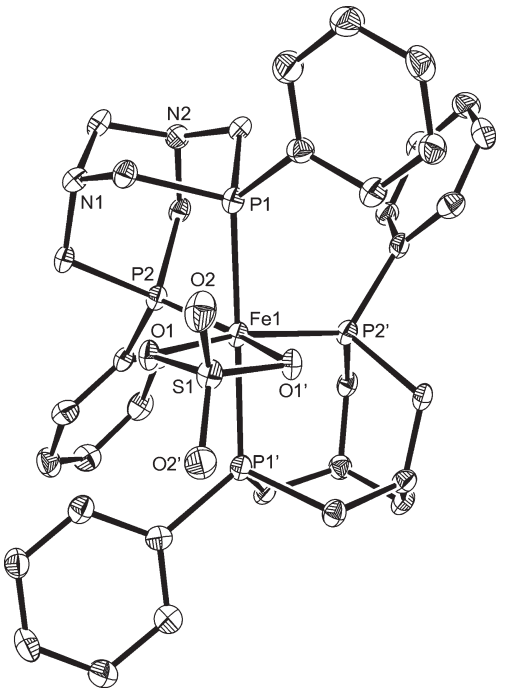

Figure 1. Molecular structure of $[Fe(\kappa^2\text{-}O_2SO_2)L_2]$ (**1**), from the crystal structure of $1\cdot 2H_2O$. Ellipsoids are represented at 30% probability. Hydrogen atoms have been omitted for clarity. Primed labels are related to those in the asymmetric unit by the $-x, y, -z + {}^1/_2$ symmetry operation.

in Figure 1. The diphosphine ligands contain a backbone of two fused 1-aza-3,5-diphosphacyclohexane rings, with the rings sharing the two nitrogen atoms and the connecting carbon atom. Each phosphorus atom is also bonded to a phenyl ring.

The two fused six-membered PN_2C_3 rings both possess chair conformations, which enables the lone pairs of the phosphorus atoms to chelate to the metal center. The crystallographic bite angle of the diphosphine in **1** is 83.42(6)°, which is close to the average values for bis-(diphenylphosphino)ethane (dppe) (85(3)°) and 1,2-bis-(diphenylphosphino)benzene (83(3)°).[1] The bite angle of the coordinated sulfate in **1** is 68.4(2)°.

The structure of **1** shows some similarities to that of $[Fe(\kappa^2\text{-}O_2SO_2)(\mathbf{L^2})]$, with two bidentate diphosphine ligands present instead of a tetradentate $\mathbf{L^2}$ ligand.[8] The Fe−P bond lengths in **1** are 2.1837(18) Å (equatorial) and 2.2831(16) Å (axial), which compares with equivalent values of 2.1803(17)/2.1776(17) Å (equatorial) and 2.2256(16)/2.2362(16) Å (axial) for $[Fe(\kappa^2\text{-}O_2SO_2)(\mathbf{L^2})]$. The lengthening of the axial Fe−P bonds with respect to the equatorial Fe−P bonds in these complexes is due to the phosphine donors having a greater *trans* influence than sulfate.

The two phenyl rings on each **L** ligand are almost perpendicular to one another, as quantified by the mean C−C···C−C torsion angle between the rings of 84°. This gives each ligand a staggered conformation, and this minimizes the steric interactions between aromatic rings of the two **L** ligands. One of the methylene groups on each **L** ligand is directed toward a ring on the other **L** ligand, and a distance of 2.54 Å between the hydrogen atom and the ring plane is suggestive of a C−H···π interaction. The included water molecules form hydrogen bonds to a

sulfate oxygen atom (O···O 2.866, H···O 2.01 Å, O−H···O 163°) and a nitrogen atom (O···N 3.047, H···N 2.20 Å, O−H···N 159°), and these link the molecules into chains.

Synthesis of *cis*-[$FeCl_2L_2$] (*cis*-2). Initial attempts to displace the coordinated sulfato ligand in **1** were unsuccessful. When [PPN]Cl (bis(triphenylphosphoranylidene)ammonium chloride) was added to a dichloromethane solution of **1**, no reaction occurred. This is in contrast to [Fe(κ^2-O_2SO_2)($\mathbf{L^2}$)], which reacts with chloride under similar conditions to form [$FeCl_2$($\mathbf{L^2}$)].[8]

To synthesize the dichloride complex [$FeCl_2\mathbf{L}_2$], iron(II) chloride and ammonium chloride (rather than the equivalent sulfate salts) were reacted with $PPh(CH_2OH)_2$ and formaldehyde. Using the same stoichiometry as with the sulfate salts, the reaction gave a similar purple precipitate as in the formation of **1**. The $^{31}P\{^1H\}$ NMR spectrum of the purple solid in $CDCl_3$ showed two triplet resonances at δ −32.4 and δ −46.5 as would be expected for a complex with the same geometry as **1**, consistent with formation of the dichloride complex *cis*-[$FeCl_2\mathbf{L}_2$] (*cis*-**2**). However, the resonances in $CDCl_3$ were broad suggesting the complex is fluxional, although cooling to 232 K failed to either sharpen the signals or resolve any additional resonances, making it unclear what fluxional processes are in operation.

Complex *cis*-**2** partially dissolves in aqueous solution to give a purple solution. When the $^{31}P\{^1H\}$ NMR spectrum was recorded in D_2O, two sharp resonances were observed at δ −17.9 and δ −38.2, although these were now observed as second order multiplets rather than triplets. The large chemical shift difference between $CDCl_3$ and D_2O is consistent with a change in the coordination sphere, and the solubility of *cis*-**2** in water at neutral pH suggests that the chloro ligands are being displaced by aqua ligands to give the dicationic complex *cis*-[$Fe(OH_2)_2\mathbf{L}_2$]Cl_2. Complex *cis*-**2** is increasingly soluble in water with decreasing pH, possibly because of protonation of the nitrogen groups. If an excess of sodium chloride is added to the aqueous solution of *cis*-[$Fe(OH_2)_2\mathbf{L}_2$]Cl_2, *cis*-**2** precipitates from solution.

Attempts to grow crystals of *cis*-**2** proved unsuccessful, though it was observed that despite the complex being largely insoluble in diethyl ether, washings of the purple solid gave a very dilute pale yellow solution. Slow evaporation of this diethyl ether solution gave yellow crystals suitable for X-ray crystallography. The resulting structure showed that this complex was *trans*-[$FeCl_2\mathbf{L}_2$] (*trans*-**2**). Because of the very low solubility of *trans*-**2** in diethyl ether, a good $^{31}P\{^1H\}$ NMR spectrum of this compound proved difficult to obtain. When dissolved in other organic solvents such as dichloromethane, chloroform, and acetone, the yellow crystals of *trans*-**2** dissolved to give a purple solution. The $^{31}P\{^1H\}$ NMR spectrum of this solution showed broad triplet resonances at δ −32.4 and δ −46.5, demonstrating that *cis*-**2** had been reformed. Dissolving *trans*-**2** in D_2O also gave a purple solution, the $^{31}P\{^1H\}$ NMR spectrum of which displayed the two multiplet resonances at δ −17.9 and δ −38.2. This suggests that the diaqua complex *cis*-[$Fe(OH_2)_2\mathbf{L}_2$]Cl_2 had formed, in a similar manner to when *cis*-**2** is dissolved in aqueous solution. The interconversions between *cis*-**2**, *trans*-**2**, and *cis*-[$Fe(OH_2)_2\mathbf{L}_2$]Cl_2 are summarized in Scheme 3.

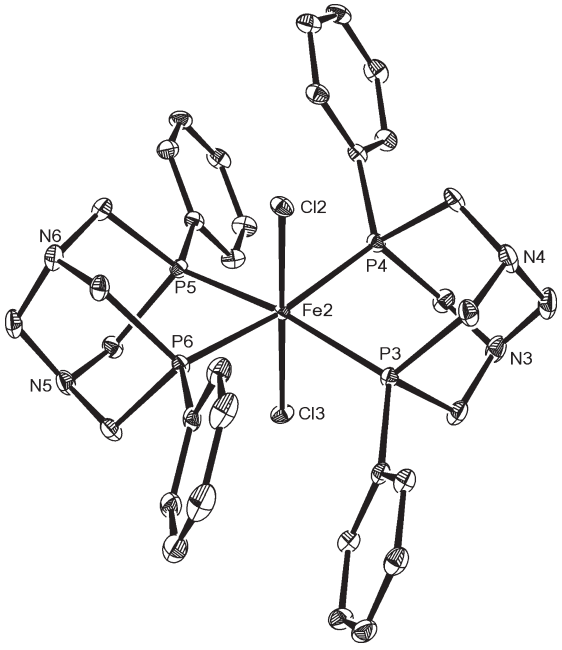

Figure 2. Molecular structure of *trans*-[$FeCl_2\mathbf{L}_2$] (*trans*-**2**), showing only the full occupancy molecule. Ellipsoids are represented at 30% probability, and hydrogen atoms have been omitted for clarity.

Scheme 3

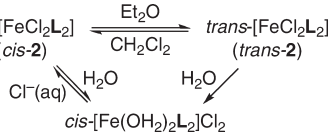

Table 3. Selected Bond Lengths (Å) and Angles (deg) for *trans*-**2**[a]

Fe(1)−P(1)	2.2674(5)	Fe(2)−P(5)	2.2614(5)
Fe(1)−P(2)	2.2954(5)	Fe(2)−P(6)	2.2506(5)
Fe(1)−Cl(1)	2.3600(4)	Fe(2)−Cl(2)	2.3676(5)
Fe(2)−P(3)	2.2469(5)	Fe(2)−Cl(3)	2.3610(5)
Fe(2)−P(4)	2.2474(5)		
P(1)−Fe(1)−P(2)	80.839(17)	P(4)−Fe(2)−P(5)	98.60(2)
P(1)−Fe(1)−P(2)′	99.161(17)	P(4)−Fe(2)−P(6)	169.13(2)
P(3)−Fe(2)−P(4)	82.007(19)	P(6)−Fe(2)−P(5)	81.669(19)
P(3)−Fe(2)−P(5)	168.17(2)	Cl(3)−Fe(2)−Cl(2)	177.47(2)
P(3)−Fe(2)−P(6)	99.98(2)		

[a] Primed atoms generated by the symmetry operation $-x, -y, -z+1$.

X-ray Crystal Structure of *trans*-[$FeCl_2\mathbf{L}_2$] (*trans*-2). The X-ray crystallographic analysis of *trans*-**2** revealed the asymmetric unit contains 1.5 molecules of the complex, with one full molecule and one-half molecule residing on a mirror plane. The full occupancy molecule is shown in Figure 2, and selected bond lengths and angles are given in Table 3. The three independent crystallographic bite angles for the diphosphine **L** ligand in the structure are 82.007(19) and 81.669(19)° for the full molecule, and 80.839(17)° for the half molecule. These are all notably lower than the value for **1** (83.42(6)°). The geometry around the metal center in *trans*-**2** is distorted from a regular octahedron, with the *cis* equatorial P−Fe−P bond angles ranging from 81.669(19) and 99.98(2)° for the full molecule and from 80.838(17) to 99.162(17)° for the half molecule. The geometry is less regular for the full molecule, with a tetrahedral distortion

present, as illustrated by a 20° angle between the two FeP_2 planes.

In the full molecule, the two phenyl rings on each of the independent **L** ligands are orientated in staggered conformations, as quantified by mean C−C···C−C torsion angles between the rings of 53° and 47°. In contrast, in the half molecule, the two phenyl rings on each ligand are almost coplanar, with a mean C−C···C−C torsion angle of 6°; hence this ligand adopts an eclipsed conformation. In both independent molecules, the phenyl groups face one another with closest C···C distances between 3.22 and 3.64 Å, consistent with the presence of intramolecular $\pi\cdots\pi$ interactions.

The six independent Fe−P bond lengths in the structure of *trans*-**2** range from 2.2469(5) to 2.2954(5) Å, and these are closer to the axial rather than the equatorial Fe−P bond lengths in the structure of **1**, as all of the Fe−P bonds in *trans*-**2** are *trans* to another phosphine. The Fe−P bond lengths in *trans*-**2** are significantly longer than those in the related bis(1,2-bis(dialkylphosphino)ethane complexes *trans*-$[FeCl_2L_2]$, where L = 1,2-bis(dimethylphosphino)ethane (2.241(1) and 2.230(1) Å),[18] 1,2-bis(diethylphosphino)ethane (2.256(2) and 2.264(2) Å), and 1,2-bis(di-*n*-propylphosphino)ethane (2.261(2) and 2.275(2) Å).[19] This is a consequence of the steric requirement of the phosphine substituents, and also the greater σ-donor ability of the trialkylphosphine donors over the dialkylarylphosphine donors in *trans*-**2**.

Reactions of *cis*-2 with Thiocyanate and Azide. Potassium thiocyanate was added to *cis*-**2** in ethanol to give an orange suspension of *cis*-$[Fe(NCS)_2\mathbf{L}_2]$ (*cis*-**3**). The $^{31}P\{^1H\}$ NMR spectrum of this complex in $CDCl_3$ showed two second order resonances at δ −31.0 and δ −38.6, as expected for a *cis* isomer, plus a singlet at δ −42.2 which was assigned to *trans*-**3**. From the integrals, the *cis* and *trans* isomers are present in a 4:1 ratio. Over time, the ratio of *cis* to *trans* isomers changes, and the $^{31}P\{^1H\}$ NMR spectrum recorded after 48 h shows a *cis*/*trans* ratio of 2:3. Orange crystals suitable for X-ray crystallography also grew over time, and these were shown to be of *trans*-**3** (see below).

The ^1H NMR spectrum of a mixture of the *cis* and *trans* isomers showed five separate AB resonances for *cis*-**3**, arising from the four inequivalent $P-CH_2-N$ methylene groups and the $N-CH_2-N$ group, and a single AB system and a singlet for *trans*-**3**. In this case the $N-CH_2-N$ methylene protons are equivalent, while each of the four $P-CH_2-N$ methylene groups is in a similar environment, with one proton axial and the other equatorial in the PN_2 six-membered rings of the diphosphine ligand.

Sodium azide was added to an ethanol solution of *cis*-**2**, resulting in a red precipitate of *cis*-$[Fe(N_3)_2\mathbf{L}_2]$ (*cis*-**4**). The $^{31}P\{^1H\}$ NMR spectrum in $CDCl_3$ showed two second order resonances at δ −27.4 and δ −36.9, assigned to *cis*-**4**, as well as a singlet at δ −43.2, assigned to *trans*-**4**, with the compounds present in an 11:1 ratio. The spectrum was unchanged after 48 h, showing that the isomerization process is less favorable for *cis*-**4** and *trans*-**4** than it is for the thiocyanate analogues. The observation of both *cis* and *trans* isomers of **4** is in contrast to the synthesis of $[Fe(N_3)_2(dmpe)_2]$ (dmpe = 1,2-bis(dimethylphosphino)ethane, which showed no evidence for the *cis* isomer, with only the *trans* isomer observed in the $^{31}P\{^1H\}$ NMR spectrum.[20]

The ^1H NMR spectrum of the mixture of *cis*-**4** and *trans*-**4** showed a similar series of resonances to that of *cis*-**3** and *trans*-**3**. Therefore, one AB system and a singlet were observed for *trans*-**4**, and five AB resonances observed for *cis*-**4**. IR spectroscopy of the mixture showed only one peak for $\nu(N_3)$ at 2043 cm^{-1}, which given the ratio of isomers observed is likely to be due to *cis*-**4**. This isomer might be expected to show both symmetric and antisymmetric stretches, though only one peak was observed for the tetraphosphine complex $[Fe(N_3)_2(\mathbf{L^1})]$, whereas the two peaks in the *cis* diazido complex $[Fe(N_3)_2\{P(CH_2CH_2PMe_2)_3\}]$ were separated by only 6 cm^{-1}.[21]

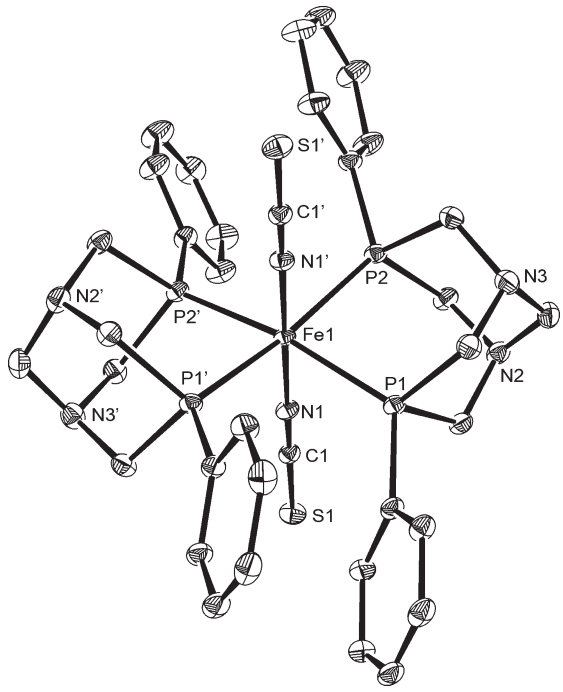

Figure 3. Molecular structure of *trans*-$[Fe(NCS)_2\mathbf{L}_2]$ (*trans*-**3**). Ellipsoids are represented at 30% probability, and hydrogen atoms have been omitted for clarity. Primed labels are related to those in the asymmetric unit by the $-x, y, -z + {}^1/_2$ symmetry operation.

Table 4. Selected Bond Lengths (Å) and Angles (deg) for *trans*-**3**[a]

Fe(1)−P(1)	2.2453(4)	N(1)−C(1)	1.165(2)
Fe(1)−P(2)	2.2592(4)	S(1)−C(1)	1.6339(16)
Fe(1)−N(1)	1.9387(14)		
P(1)−Fe(1)−P(2)	82.469(15)	N(1)′−Fe(1)−N(1)	179.20(8)
P(1)−Fe(1)−P(1)′	98.24(2)	C(1)−N(1)−Fe(1)	177.58(12)
P(1)′−Fe(1)−P(2)	166.572(15)	N(1)−C(1)−S(1)	179.50(16)
P(2)−Fe(1)−P(2)′	99.97(2)		

[a] Primed atoms generated by the symmetry operation $-x, y, -z + {}^1/_2$.

X-ray Crystal Structure of *trans*-$[Fe(NCS)_2\mathbf{L}_2]$ (*trans*-3). The X-ray analysis of the orange crystals isolated from

(18) Di Vaira, M.; Midollini, S.; Sacconi, L. *Inorg. Chem.* **1981**, *20*, 3430–3435.
(19) Baker, M. V.; Field, L. D.; Hambley, T. W. *Inorg. Chem.* **1988**, *27*, 2872–2876.
(20) Field, L. D.; George, A. V.; Pike, S. R.; Buys, I. E.; Hambley, T. W. *Polyhedron* **1995**, *14*, 3133–3137.
(21) Field, L. D.; Messerle, B. A.; Smernik, R. J. *Inorg. Chem.* **1997**, *36*, 5984–5990.

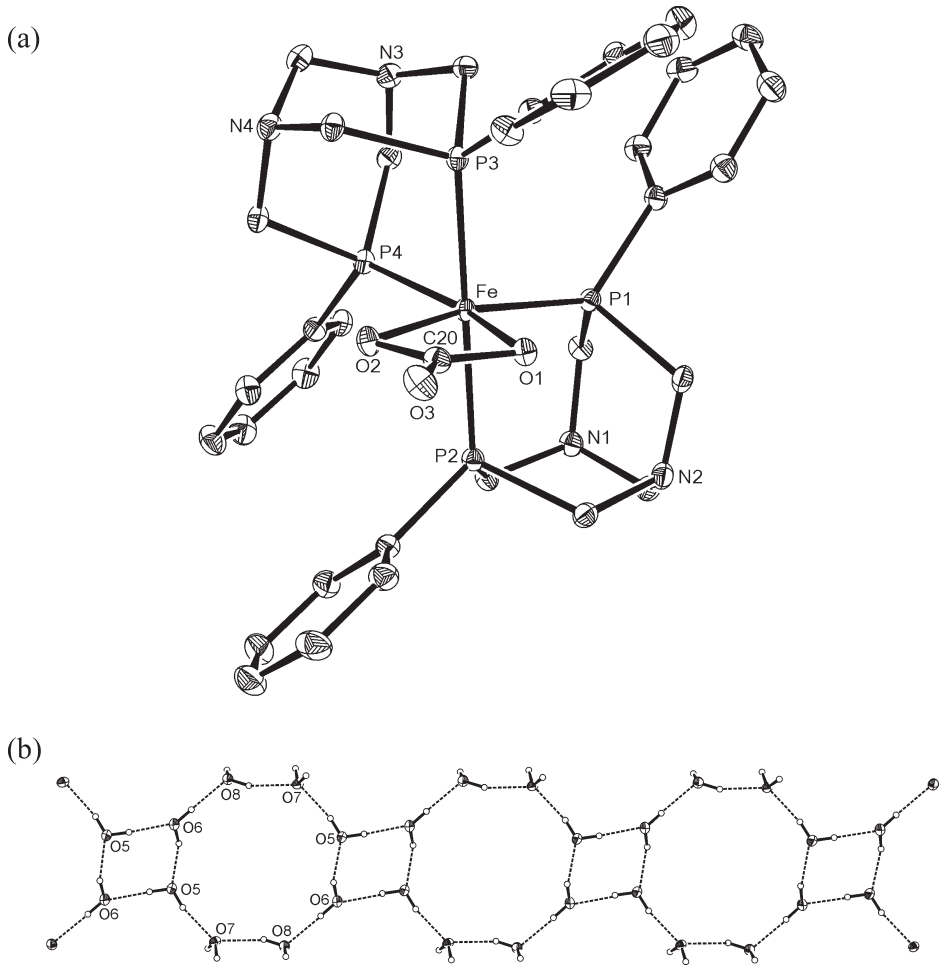

Figure 4. (a) Molecular structure of $[Fe(\kappa^2\text{-}O_2CO)\mathbf{L}_2]$ (**5**), from the crystal structure of $\mathbf{5}\cdot 7H_2O$. Ellipsoids are represented at 30% probability. Hydrogen atoms have been omitted for clarity. (b) The hydrogen-bonded tapes of water molecules present in the structure of $\mathbf{5}\cdot 7H_2O$.

the $CDCl_3$ solution containing *cis*- and *trans*-**3** showed the structure to be of *trans*-**3**, as shown in Figure 3. The asymmetric unit of the structure contains one-half molecule of *trans*-**3**, with the other generated by symmetry inherent to the space group. Selected bond lengths and angles for *trans*-**3** are given in Table 4. The thiocyanato ligands are coordinated to the iron center by the nitrogen atoms, in a similar manner to that observed in the tetraphosphine complex $[Fe(NCS)_2(\mathbf{L^1})]$.[8] The thiocyanato ligands in *trans*-**3** are almost linear, with the Fe−N−C angle 177.58(12)°.

The conformation adopted by *trans*-**3** is similar to that of the full molecule in the crystal structure of *trans*-**2**. There is a tetrahedral distortion around the iron center, with the angle between the two FeP_2 planes being 20°. The two phenyl rings within each **L** ligand are staggered with respect to each other (mean C−C···C−C torsion angle 46°), and face the equivalent phenyl group on the other **L** ligand. The shortest distance between the phenyl rings of the two **L** ligands is 3.3 Å, suggesting the presence of $\pi\cdots\pi$ interactions. Phenyl rings on adjacent molecules also interdigitate parallel to each other, but the longer distance between them suggests this occurs for packing reasons rather than as the consequence of any significant $\pi\cdots\pi$ interactions.

Reaction of *cis*-2 with Carbonate. The reaction of an ethanol solution of *cis*-**2** with an aqueous solution of sodium carbonate gave a pink suspension of $[Fe(\kappa^2\text{-}O_2CO)\mathbf{L}_2]$ (**5**). The $^{31}P\{^1H\}$ NMR spectrum of **5** in $CDCl_3$ showed two triplet resonances at δ −20.2 and δ −41.4 with $^2J_{PP}$ 72 Hz. The ^1H NMR spectrum of **5** showed the expected pattern for a bis(diphosphine) complex possessing *cis* geometry, that is, four AB systems for the P−CH_2−N methylene protons and one AB system for the N−CH_2−N methylene protons. The N−CH_2−N protons give rise to the second order AB system centered at δ 3.9, with the four remaining P−CH_2−N methylene proton groups giving four sets of AB systems between δ 5.2 and δ 2.6, some of which overlap.

X-ray Crystal Structure of $[Fe(\kappa^2\text{-}O_2CO)\mathbf{L}_2]\cdot 7H_2O$ ($\mathbf{5}\cdot 7H_2O$). Purple crystals were grown from the slow evaporation of an aqueous solution of **5** over 8 weeks, and were shown by a single crystal X-ray analysis to be the heptahydrate. The structure confirms that the two chloro ligands have been replaced with a bidentate carbonate, giving a *cis* octahedral geometry as shown in Figure 4a. Selected bond lengths and angles are given in Table 5. The chelating carbonato ligand has a small bite angle, which results in a structure that is far from a regular octahedral geometry. The *cis* equatorial bond angles range between 65.00(9)° and 100.98(4)°. The crystallographic bite angles of the diphosphine ligand in the structure are 82.62(3)° and 82.88(4)°, which are similar to those in complexes **1**, *trans*-**2** and *trans*-**3**. In comparison with the X-ray structure of $[Fe(\kappa^2\text{-}O_2CO)(\mathbf{L^1})]$,[8] the Fe−O bonds are similar (2.030(2)

Table 5. Selected Bond Lengths (Å) and Angles (deg) for $5 \cdot 7H_2O$

Fe−P(1)	2.2045(9)	Fe−O(2)	2.016(2)
Fe−P(2)	2.2630(10)	C(20)−O(1)	1.316(4)
Fe−P(3)	2.2572(10)	C(20)−O(2)	1.315(4)
Fe−P(4)	2.1911(9)	C(20)−O(3)	1.247(4)
Fe−O(1)	2.030(2)		
P(1)−Fe-P(2)	82.62(3)	P(4)−Fe-P(2)	99.77(4)
P(4)−Fe-P(3)	82.88(4)	O(2)−Fe-O(1)	65.00(9)
P(1)−Fe-P(3)	99.25(4)	O(3)−C(20)−O(1)	124.8(3)
P(4)−Fe-P(1)	100.98(4)	O(3)−C(20)−O(2)	123.8(3)
P(3)−Fe-P(2)	176.45(4)	O(2)−C(20)−O(1)	111.5(3)

and 2.016(2) Å for $5 \cdot 7H_2O$ compared to 2.044(5) and 2.073(5) Å for [Fe(κ^2-O_2CO)($\mathbf{L^1}$)]). The O−Fe−O bite angle in $5 \cdot 7H_2O$ (65.00(9)°) is larger than that of [Fe(κ^2-O_2CO)($\mathbf{L^1}$)] (63.8(2) Å). In contrast to **1**, the two independent **L** ligands adopt conformations in which the two phenyl rings are almost coplanar, as quantified by mean C−C···C−C torsion angles of 7° and 13° for the two ligands.

The related complex [Fe(κ^2-O_2CO)(dmpe)$_2$] has been recently reported from the reaction between *trans*-[$FeMe_2$(dmpe)$_2$] and CO_2, probably in the presence of adventitious water.[22] This compound crystallizes as a H_2CO_3 adduct, with a pair of hydrogen bonds between the carbonic acid molecule and the coordinated carbonate. The Fe−O distances are comparable with those in $5 \cdot 7H_2O$ (2.039(2), 2.041(2) Å), whereas the O−Fe−O bite angle is slightly lower (64.48(9)°).

Unsurprisingly, the included water molecules in the structure of $5 \cdot 7H_2O$ are involved in hydrogen bonding, with the carbonate oxygen atoms and the **L** nitrogen atoms both acting as acceptors. In addition, there are tapes formed by hydrogen-bonded water molecules running through the lattice. These tapes contain alternating eight- and four-membered rings (T4(2)8(2)),[23] as shown in Figure 4b. Water molecules can adopt a multitude of hydrogen-bonding arrangements within crystal structures, but this motif is relatively unusual with only a few previous examples.[24]

Reaction of *cis*-2 with CO. When CO was bubbled through an aqueous solution of *cis*-**2**, the color changed over an hour from purple to yellow. The $^{31}P\{^1H\}$ NMR spectrum of the yellow solution showed a singlet resonance at δ −51.0, consistent with formation of a *trans* bis(diphosphine) complex, *trans*-**6**. ^1H NMR spectroscopy showed two sets of AB doublets at δ 4.9 and δ 4.4, and δ 3.8 and δ 3.5, as well as a singlet at δ 3.9. This indicates that *trans*-**6** is unsymmetrically substituted, since the ^1H NMR spectrum of a symmetrical product such as *trans*-[Fe(CO)$_2$**L**$_2$]$^{2+}$ would give a single AB system and a singlet in a 4:1 ratio because the four P−CH_2−N methylene groups on each **L** ligand would be equivalent.

When the reaction was repeated with ^{13}CO a similar yellow solution was produced, but now the $^{31}P\{^1H\}$ NMR spectrum showed a doublet at δ −51.1 with $^2J_{PC}$ 25.8 Hz. The doublet indicates that only one ^{13}CO ligand is bound to the iron center. The $^{13}C\{^1H\}$ NMR spectrum is consistent with this, showing a quintet ^{13}CO resonance at δ 214.7. The IR spectrum of *trans*-**6** showed a single ^{12}CO stretching frequency at 1939 cm^{-1}, which would be expected for a monocarbonyl complex. The IR spectrum of the corresponding ^{13}CO complex showed the equivalent ^{13}CO stretching frequency with the expected isotopic shift at 1895 cm^{-1}. The ESI mass spectrum showed the major peak to be at m/z 747.1, which can be assigned to the chloride carbonyl complex cation [FeCl(CO)**L**$_2$]$^+$. As a result of the combined spectroscopic evidence, *trans*-**6** has been identified as *trans*-[FeCl(CO)**L**$_2$]Cl.

Scheme 4

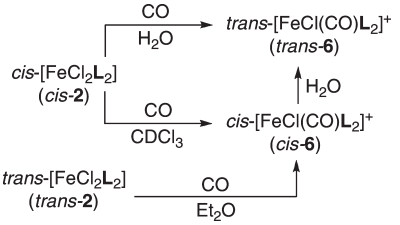

When the reaction between *cis*-**2** and CO was carried out in $CDCl_3$, the $^{31}P\{^1H\}$ NMR spectrum showed four main resonances at δ −39.4, δ −55.3, δ −59.4, and δ −69.0, which are all doublets of doublets of doublets, though the resonance at δ −69.0 appears simpler because of two of the $^2J_{PP}$ values being coincidently similar. The coupling pattern shows that all four phosphorus donors in the complex are inequivalent, strongly suggesting that the product is *cis*-[FeCl(CO)**L**$_2$]Cl (*cis*-**6**). This formulation was strongly supported by the $^{13}C\{^1H\}$ NMR spectrum recorded upon reaction with ^{13}CO rather than ^{12}CO, the spectrum displaying a single multiplet carbonyl resonance at δ 214.1. On leaving this solution to stand at room temperature, a small quantity of *trans*-**6** appeared, as witnessed by a doublet ^{31}P resonance (δ −51.0) and quintet ^{13}CO resonance, but this remained a minor product, with no evidence for an equilibrium between the isomers.

When *trans*-**2** was reacted with CO in diethyl ether solution, a pale orange precipitate was formed. The $^{31}P\{^1H\}$ NMR spectrum of the orange solid dissolved in $CDCl_3$ showed the product to be *cis*-**6**. When *cis*-**6** was dissolved in D_2O, it gave a yellow solution and the $^{31}P\{^1H\}$ NMR spectrum showed a singlet resonance at δ −51.0. This is similar to the spectrum observed for *trans*-**6**, suggesting that *cis*-**6** isomerizes in water.

The syntheses and interconversions of **6** are summarized in Scheme 4. While the formation of *cis*-**6** in Et_2O is likely to be driven by solubility, it is noteworthy that the majority of reactions in water lead to isomerization. It is likely that these processes occur via initial coordination of H_2O, though the reactions are too fast to obtain spectroscopic evidence to validate this.

Another example of how the geometrical isomer isolated is influenced by reaction conditions is provided by Mays and co-workers.[25] When *trans*-[$FeCl_2$(dmpe)$_2$] was reacted with CO in an acetone solution in the presence of $NaBPh_4$, *cis*-[FeCl(CO)(dmpe)$_2$]BPh_4 was formed as the major product. In contrast, when *trans*-[$FeCl_2$(dmpe)$_2$]

(22) Allen, O. R.; Dalgarno, S. J.; Field, L. D.; Jensen, P.; Turnbull, A. J.; Willis, A. C. *Organometallics* **2008**, *27*, 2092–2098.

(23) Infantes, L.; Chisholm, J.; Motherwell, S. *CrystEngComm* **2003**, *5*, 480–486. Mascal, M.; Infantes, L.; Chisholm, J. *Angew. Chem., Int. Ed.* **2006**, *45*, 32–36.

(24) Wang, J.; Hu, S.; Tong, M.-L. *Eur. J. Inorg. Chem.* **2006**, 2069–2077. Fan, G.; Xie, G.; Chen, S.; Gao, S. *J. Coord. Chem.* **2007**, *60*, 1093–1099.

(25) Bellerby, J. M.; Mays, M. J.; Sears, P. L. *J. Chem. Soc., Dalton Trans.* **1976**, 1232–1236.

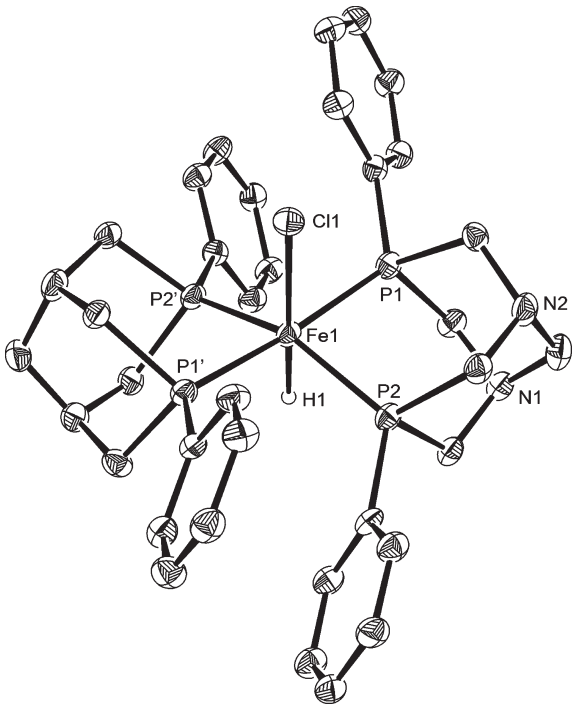

Figure 5. Molecular structure of *trans*-[FeCl(H)$\mathbf{L}_2$] (**7**), from the crystal structure of **7**·1.5C_6H_6. Only one of the independent complex molecules is shown. Ellipsoids are represented at 30% probability. With the exception of the hydride ligand, hydrogen atoms have been omitted for clarity. Primed labels are related to those in the asymmetric unit by the $-x$, y, $-z + {}^1/_2$ symmetry operation.

was reacted with CO in a refluxing acetone solution for 5 h, followed by addition of $NaBPh_4$, the major product was *trans*-[FeCl(CO)(dmpe)$_2$]BPh_4. In both cases, the other isomer was observed as a minor product, but in this system no evidence was observed for the interconversion of the isomers in solution.

Reaction of *cis*-2 with Sodium Borohydride. When *cis*-**2** and 2 equiv of sodium borohydride were dissolved in ethanol under a nitrogen atmosphere, an orange solution formed, which produced an orange precipitate after 1 h. The reaction mixture was stirred at room temperature for a further 1 h to complete the reaction, then the crude material was separated by filtration and recrystallized from degassed benzene to give *trans*-[FeCl(H)$\mathbf{L}_2$] (**7**) as a dark orange microcrystalline solid.

The $^{31}P\{^1H\}$ NMR spectrum of **7** in C_6D_6 showed a singlet at δ −27.5 consistent with a *trans* complex. When the same ^{31}P NMR experiment was run without proton decoupling, the singlet split into a doublet with $^2J_{PH}$ 49 Hz, suggesting the phosphorus resonance is coupling to a single hydride nucleus. The ^1H NMR spectrum of the solid dissolved in C_6D_6 showed a quintet at δ −28.6 because of the coupling of the hydride with the four equivalent phosphorus nuclei, confirming the presence of the hydride in the complex and the *trans* geometry.

These observations are similar to those reported by the groups of Tyler and Holah for the related compounds *trans*-[FeCl(H)(bmppe)$_2$] (bmppe = 1,2-bis(bis-(methoxypropyl)phosphino)ethane) and *trans*-[FeCl(H)(dppm)$_2$] (dppm = bis(diphenylphosphino)methane). These compounds both displayed low frequency quintet hydride resonances (δ −31.8 and δ −21.2, respectively), with $^2J_{PH}$ values of 45−46 Hz.[26] Complex **7** proved to be relatively air-stable in the solid-state, showing no change after 24 h. In contrast, ethanolic solutions of **7** turned brown and decomposed upon exposure to air after a few minutes.

Table 6. Selected Bond Lengths (Å) and Angles (deg) for **7**·1.5C_6H_6[a]

Fe(1)−P(1)	2.2050(14)	Fe(2)−P(4)	2.2075(15)
Fe(1)−P(2)	2.1595(13)	Fe(1)−Cl(1)	2.461(2)
Fe(2)−P(3)	2.1708(14)	Fe(2)−Cl(2)	2.454(2)
P(2)−Fe(1)−P(1)	83.59(5)	P(2)′−Fe(1)−P(1)	98.20(5)
P(3)−Fe(2)−P(4)	83.13(5)	P(3)−Fe(2)−P(4)′	98.22(5)
P(1)−Fe(1)−P(1)′	172.16(9)	P(1)−Fe(1)−Cl(1)	86.08(4)
P(2)−Fe(1)−P(2)′	153.72(9)	P(2)−Fe(1)−Cl(1)	103.14(5)
P(3)−Fe(2)−P(3)′	154.44(10)	P(3)−Fe(2)−Cl(2)	102.78(5)
P(4)′−Fe(2)−P(4)	173.99(9)	P(4)−Fe(2)−Cl(2)	86.99(5)

[a] Primed atoms generated by the symmetry operation $-x$, y, $-z + {}^1/_2$.

X-ray Crystal Structure of *trans*-[FeCl(H)$\mathbf{L}_2$]·1.5$\mathbf{C_6H_6}$ (7·1.5$\mathbf{C_6H_6}$). Orange crystals from the recrystallization of **7** in benzene were suitable for single crystal analysis. The asymmetric unit contains two independent half molecules of *trans*-[FeCl(H)$\mathbf{L}_2$] along with one-half molecule of benzene with full occupancy and one whole molecule of benzene exhibiting 1:1 disorder. One of independent complex molecules is shown in Figure 5. Selected bond lengths and angles are given in Table 6.

The two Fe−Cl bond lengths in the structure are 2.461(2) and 2.454(2) Å for the Fe(1)−Cl(1) and Fe(1)−Cl(2) bonds, respectively, which are significantly longer than those observed in *trans*-**2** because of increased *trans* influence of hydride relative to chloride. Only two other X-ray crystal structures of similar complexes of the formula *trans*-[FeCl(H)L_2] (where L = any bidentate phosphine ligand) have been reported in the literature to date. Both of these have slightly shorter Fe−Cl bond lengths than **7**, 2.404(2) Å for *trans*-[FeCl(H)(dppe)$_2$][27] and 2.4044(12) Å for *trans*-[FeCl(H)(depe)$_2$] (depe = bis-(diethylphosphino)ethane).[28]

The conformations of the two independent molecules in the structure of **7** are similar to the full molecule of complex *trans*-**2**. Within each **L** ligand, the two phenyl rings are staggered with respect to each other, as quantified by C−C···C−C torsion angles of 47−50°. The iron centers are distorted octahedral, with two of the phosphorus centers on each molecule pushed toward the hydride, giving *trans* P−Fe−P angles of 154°. The pairs of phenyl rings on the two **L** ligands within each complex molecule are approximately parallel, and closest C···C contacts of 3.3 Å suggest the presence of $\pi\cdots\pi$ interactions. In the supramolecular structure, the molecules are aligned into chains, with the chloride of one complex directed to the hydride of a neighbor, though this is likely to be the consequence of packing as opposed to any interaction.

Electrochemistry. Cyclic voltammetry studies were carried out on **1**, *cis*-**2**, and **7** to determine their redox

(26) Gao, Y.; Holah, D. G.; Hughes, A. N.; Spivak, G. J.; Havighurst, M. D.; Magnuson, V. R.; Polyakov, V. *Polyhedron* **1997**, *16*, 2797–2807. Gilbertson, J. D.; Szymczak, N. K.; Crossland, J. L.; Miller, W. K.; Lyon, D. K.; Foxman, B. M.; Davis, J.; Tyler, D. R. *Inorg. Chem.* **2007**, *46*, 1205–1214.

(27) Lee, J.-G.; Jung, G.-S.; Lee, S. W. *Bull. Korean Chem. Soc.* **1998**, *19*, 267–269.

(28) Wiesler, B.; Tuczek, F.; Näther, C.; Bensch, W. *Acta Crystallogr., Sect. C* **1998**, *54*, 44–46.

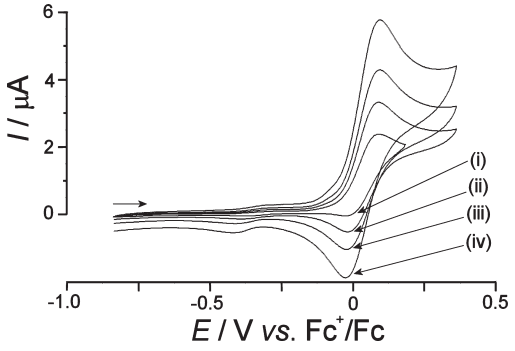

Figure 6. Cyclic voltammograms for the oxidation of 1 mM [Fe(κ^2-O_2SO_2)$\mathbf{L}_2$] (**1**) at a 1 mm diameter Pt electrode in 1,2-dichloroethane/0.1 M NBu_4PF_6 at scan rates of (i) 20 mV s^{-1}, (ii) 50 mV s^{-1}, (iii) 100 mV s^{-1}, and (iv) 200 mV s^{-1}.

properties, as well as to establish whether the related iron(III) complexes were stable and potentially isolable. Cyclic voltammograms were recorded using a 1 mm platinum electrode and employed 1 mM 1,2-dichloroethane solutions of the complexes with 0.1 M tetrabutylammonium hexafluorophosphate as the electrolyte. In the case of **1**, the voltammogram recorded with an initial scan rate of 20 mV s^{-1} showed a chemically irreversible peak at about 0 V versus Fc^+/Fc (see Figure 6), which suggests that the complex is reactive upon oxidation. Voltammograms were then recorded at 50, 100, and 200 mV s^{-1}, and the Fe(II)/Fe(III) redox process was seen to become more reversible with increasing scan rate. The small redox process at −0.4 V versus Fc^+/Fc is believed to be a result of either a minor impurity or a new species resulting from the decomposition of **1**. Insolubility of **1** in acetonitrile prevented the cyclic voltammetry being investigated in that solvent.

The voltammogram for *cis*-**2** in 1,2-dichloroethane was first recorded at 200 mV s^{-1}, which showed the main reversible process at −0.35 V versus Fc^+/Fc. A second but minor process was observed at −0.05 V versus Fc^+/Fc. When the voltammogram of *cis*-**2** was obtained at lower scan rates, both reversible redox processes were still observed in the same ratio, suggesting that two isomers may be present in solution. Unlike the sulfate complex **1**, the dichloride complex [$FeCl_2\mathbf{L}_2$] can switch between *cis* and *trans* isomers. As the purple *cis*-**2** was used in the experiment and the 1,2-dichloroethane solution was purple, it seems highly likely that the main Fe(II)/Fe(III) redox process at −0.35 V versus Fc^+/Fc is associated with *cis*-**2**. As the Fe(II)/Fe(III) redox process for *cis*-**2** occurs at a more negative potential than for **1**, it can be concluded that the dichloride complex *cis*-**2** is easier to oxidize than the sulfate complex **1**. The minor redox process at 0.05 V versus Fc^+/Fc can be tentatively assigned as arising from complex *trans*-**2**. Cyclic voltammetry of *trans*-**2** in 1,2-dichloroethane would be ideal for comparison, but the complex converted rapidly to *cis*-**2** in this solvent, as indicated by the deep purple coloration of the solution when yellow crystals of *trans*-**2** were dissolved. Cyclic voltammetry studies of *cis*-**2** were also carried out in acetonitrile. The CV (scan rate = 100 mV s^{-1}) now showed only one reversible redox process at −0.35 V versus Fc^+/Fc due to *cis*-**2**. No redox process at about −0.1 V versus Fc^+/Fc was observed in the voltammogram, that is, there

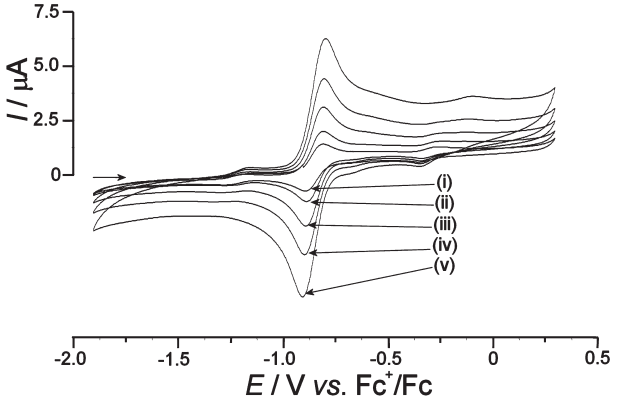

Figure 7. Cyclic voltammograms for the oxidation of 1 mM *trans*-[FeCl(H)$\mathbf{L}_2$] (**7**) at a 1 mm diameter Pt electrode in 1,2-dichloroethane/0.1 M NBu_4PF_6 at scan rates of (i) 10 mV s^{-1}, (ii) 20 mV s^{-1}, (iii) 50 mV s^{-1}, (iv) 100 mV s^{-1}, and (v) 200 mV s^{-1}.

appeared to be no appearance of *trans*-**2**. This suggests that the complex stays as the *cis* isomer in acetonitrile solution, which is consistent with the greater polarity of acetonitrile than 1,2-dichloroethane.

The voltammogram obtained for **7** showed one main oxidation process occurring at −0.85 V versus Fc^+/Fc, which can be assigned to the Fe(II)/Fe(III) redox process for the *trans* hydride chloride complex **7**. The experiment was repeated at scan rates of 20, 50, 100, and 200 mV s^{-1} (Figure 7), indicating fully reversible characteristics. Therefore, the iron(III) complex [FeCl(H)$\mathbf{L}_2$]$^+$ is stable even at low scan rates, making it a rare example of a stable 17-electron metal(III) hydride complex formed from the oxidation of the corresponding neutral 18-electron species.[29] After leaving the 1,2-dichloroethane solution of **7** for 30 min under argon, the color of the solution changed from bright orange to a darker orange/purple, and the voltammogram showed two new processes at −1.25 and −0.35 V versus Fc^+/Fc. Both processes appear reversible, but were not fully identified. The process at −0.35 V versus Fc^+/Fc occurs at the same potential as *cis*-**2** in 1, 2-dichloroethane, suggesting the process could be caused by this complex, which may be present as a decomposition product. The observed darkening of the solution supports this interpretation. Additionally, the more negative potential of the hydride complex **7** compared to that of *cis*-**2** shows that **7** is far easier to oxidize than *cis*-**2**, which would be expected for a hydride complex.

Conclusions

The reaction between $PPh(CH_2OH)_2$, NH_4^+, and formaldehyde in the presence of iron(II) salts has led to the formation of the iron(II) complexes [Fe(κ^2-O_2SO_2)$\mathbf{L}_2$] (**1**) and *cis*-[$FeCl_2\mathbf{L}_2$] (*cis*-**2**) which contain the novel self-assembled 3,7-diphenyl-1,5-diaza-3,7-diphosphabicyclo[3.3.1]-nonane ligand **L**. This is the first observation of a diphosphine containing the 1,5-diaza-3,7-diphosphabicyclo-[3.3.1]nonane backbone, and the product is in marked contrast to that observed from the related reaction between $P(CH_2OH)_4^+$, NH_4^+, and iron(II). This demonstrates how the use of hydroxymethylphosphines can give rise to unusual

(29) Hamon, P.; Toupet, L.; Hamon, J.-R.; Lapinte, C. *Organometallics* **1992**, *11*, 1429–1431.

and unprecedented structural types through self-assembly reactions. The iron(II) center is necessary for the formation of **L**, and the reaction of $PPh(CH_2OH)_2$, NH_4^+, and formaldehyde without iron(II) gives multiple products that could not be unambiguously characterized. The chloro ligands in the complex *cis*-$[FeCl_2\mathbf{L}_2]$ can readily be substituted, and both *cis* and *trans* isomers of compounds of the general formula $[FeX_2\mathbf{L}_2]$ have been observed and in some cases can be interconverted. Current work is focused on removing **L** from the metal template for reaction with other metal centers and studying the 17-electron iron(III) complexes.

Acknowledgment. We thank the EPSRC for financial support (Doctoral Training Award to A.S.K.).

Supporting Information Available: Crystallographic information files (CIF) for the structures of $\mathbf{1}\cdot 2H_2O$, *trans*-**2**, *trans*-**3**, $\mathbf{5}\cdot 7H_2O$, and $\mathbf{7}\cdot 1.5C_6H_6$. This material is available free of charge via the Internet at http://pubs.acs.org.